RESEARCH ARTICLE

Regulation of Cell Cycle Components During Exposure to Anoxia or Dehydration Stress in the Wood Frog, *Rana sylvatica*

JOURNAL OF EXPERIMENTAL ZOOLOGY
PART A
ECOLOGICAL GENETICS AND PHYSIOLOGY
A Journal of Integrative Biology

RABIH ROUFAYEL, KYLE K. BIGGAR, AND KENNETH B. STOREY*
Institute of Biochemistry and Department of Biology, Carleton University, Ottawa, Ontario, Canada

ABSTRACT

The wood frog (*Rana sylvatica*) exhibits a well-developed natural anoxia and dehydration tolerance. The degree of stress tolerance depends on numerous biochemical adaptations, including stress-induced hypometabolism that helps to preserve long-term viability by reducing ATP demand. We hypothesized that the mechanisms involved in cell cycle control could act to aid in the establishment of the hypometabolic state required for stress survival. Selected proteins involved in the proliferation of cells were evaluated using immunoblotting in liver and skeletal muscle of wood frogs comparing controls with animals subjected to either 24-hr anoxia exposure under a nitrogen gas atmosphere or dehydration to 40% of total body water lost (all at 5°C). Levels of cyclins (type A, B, D, and E) decreased significantly under both stresses in liver and skeletal muscle. Similar reductions were seen for Cyclin-dependant kinases (Cdk) types 2, 4, and 6 in both liver and skeletal muscle; however, an increase in the relative amount of phosphorylated inactive p-Cdk (Thr14/Tyr15) was observed in liver under both stresses. Levels of positive regulators of Cdk activity (Cdc25 type A and C) were significantly reduced in both tissues under both stresses, whereas negative regulators of Cdk activity ($p16^{INK4a}$ and $p27^{KIP1}$) increased significantly in liver under both anoxia and dehydration stress (but not in muscle). This study provides the first report of differential regulation of cell cycle components in an anoxia and dehydration tolerant vertebrate, the wood frog, suggesting that cell cycle suppression is an active part of stress resistance and life extension in hypometabolic states. *J. Exp. Zool. 315:487–494, 2011.* © 2011 Wiley-Liss, Inc.

How to cite this article: Roufayel R, Biggar KK, Storey KB. 2011. Regulation of cell cycle components during exposure to anoxia or dehydration stress in the wood frog, *Rana sylvatica*. J. Exp. Zool. 315:487–494.

J. Exp. Zool. 315:487–494, 2011

Many amphibians live in habitats where they experience wide variation in environmental parameters including oxygen and water availability and temperature change. To deal with these stresses, they have developed a range of biochemical and physiological adaptations that aid long-term survival. For example, underwater hibernation in ice-locked ponds/lakes often imposes long-term hypoxia or anoxia, whereas the water permeable skin of amphibians makes them highly susceptible to desiccation whenever they are on land (Hillman et al., 2009). Some species that hibernate on land even have the remarkable ability to endure whole body freezing during the winter (Storey and Storey, 2004a). The North American wood frog, *Rana sylvatica*, displays all these capabilities: well-developed anoxia resistance (at least 48 hr under N_2 gas atmosphere at 5°C), the ability to endure the loss of about 60% of total body water, and freeze tolerance (Churchill and Storey, '94; Holden and Storey, '97; Storey and Storey, 2004a). Understanding how vertebrates deal naturally with these stresses can have important biomedical implications, especially with respect to low oxygen and low water

Grant Sponsor: Natural Sciences and Engineering Research Council (NSERC) of Canada; Grant number: 6793.

*Correspondence to: Kenneth B. Storey, Institute of Biochemistry and Department of Biology, Carleton University, 1125 Colonel By Drive, Ottawa, Ontarion, Canada K1S 5B6. E-mail: kenneth_storey@carleton.ca

Received 16 March 2011; Revised 10 May 2011; Accepted 23 May 2011
Published online 27 July 2011 in Wiley Online Library (wileyonlinelibrary.com). DOI: 10.1002/jez.696

tolerances that are very well-developed in most amphibians but poor in mammals (including man).

A key component of stress tolerance in lower vertebrates is metabolic rate depression that lowers cell/tissue ATP demand when environmental conditions are incompatible with normal life and thereby extends the time that animals can survive using only endogenous fuel and energy reserves (Storey and Storey, 2004b). One part of energy conservation comes from a reduction of various physiological activities (heart beat, breathing, muscle movements, etc.) but, on the molecular scale, many intracellular energy-expensive enzymes, pathways and functions are specifically targeted and strongly suppressed (Storey and Storey, 2004b, 2007). One of the most energy-expensive activities that organisms undertake is the proliferation of cells to support growth or development and to replace damaged cells (Mazia, '62). Therefore, we hypothesized that cell cycle arrest would be a very important component of global metabolic rate depression as a survival strategy for dealing with anoxia or dehydration stresses.

Uncontrollable cellular proliferation and hypoxic tumor progression are linked in vertebrate tissues, and are often associated with mild dehydration stresses (Dalal and Bruera, 2004; Semenza, 2007). Consequently, studies of the molecular mechanisms controlling these processes in an anoxia- and dehydration-tolerant vertebrate can have significant clinical applications. We proposed that exposure to anoxia or dehydration stresses would alter or disrupt the cell cycle to facilitate metabolic rate suppression and enhance long-term stress survival.

Cellular proliferation is an extremely complex process that responds to a wide variety of extracellular and intracellular signals and stressors. Progression through the cell cycle is tightly regulated by Cyclin-dependent kinases (Cdks) whose activity is dependent on binding to regulatory proteins, called cyclins. Growth factors trigger signal cascades that lead to sequential activation of Cdks and these activated Cdks are the main driving force behind the cell cycle (Obaya and Sedivy, 2002; Harrisingh et al., 2004; Guardavaccaro and Pagano, 2006). Cdk activation is regulated by several mechanisms including binding of a cyclin regulatory subunit, dephosphorylation of conserved inhibitory sites (Thr14 or Tyr15) by cell division cycle 25 phosphatases (Cdc25 type A and C), or binding Cdk inhibitor proteins including $p16^{INK4a}$ and $p27^{KIP1}$ (Fig. 1) (Pavletich, '99; Welburn et al., 2007).

To examine the responses of cell cycle to both anoxia and dehydration stresses in wood frog organs, this study examines the comparative amount of several proteins involved in cell cycle regulation including Cdks (types 1, 2, 4, and 6), cyclins (types A, B, D, and E) and several Cdk regulators (Cdc25A, Cdc25C, $p16^{INK4a}$, and $p27^{KIP1}$). Analysis of these proteins yielded a broad picture of the status of the cell cycle as well as its regulation and adaptation during metabolic rate depression in wood frog skeletal muscle and liver.

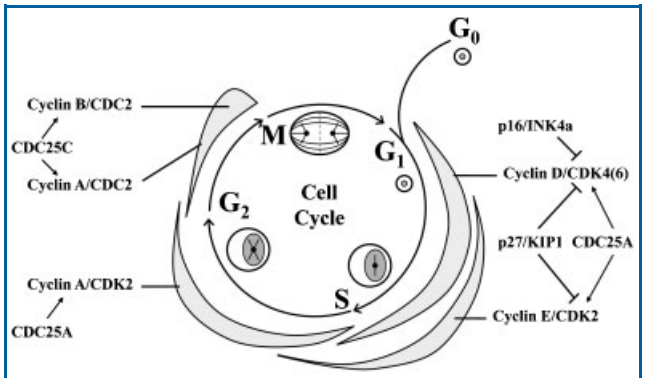

Figure 1. Expression profiles of cyclin:Cdk complexes and select Cdk regulators throughout the cell cycle. Cyclic expression of these complexes allow for the completion of one phase before the initiation of the subsequent phase. This series of events is collectively referred to as the cell cycle.

MATERIALS AND METHODS

Animals

Mature male wood frogs, *R. sylvatica*, were collected from breeding ponds in the Ottawa area in mid-April. Animals were washed in a tetracycline bath and held in the laboratory at 5 ± 1°C for at least 1 week before use. Control frogs were sampled from this condition. For the anoxia exposure experiments, the protocol of Holden and Storey ('97) was used. Plastic jars (700 mL) were used as experimental containers; these had two syringe ports in the lid to introduce and vent nitrogen gas. Jars were lined on the bottom with damp paper toweling (wetted using water that had been previously bubbled with 100% nitrogen gas for 20 min) and then the jars were flushed with N_2 gas for 15–20 min. Frogs were placed in the jars (five to six frogs in each) and then lids were secured and sealed with parafilm. The jars were flushed again with nitrogen gas for 30 min while held on ice throughout. Syringe ports were then capped and jars were replaced in the 5 ± 1°C incubator for 24 hr. Following this, the jars were transferred back to the crushed ice bath and N_2 gassing was restarted to maintain the anoxic atmosphere while the frogs were quickly sampled.

Dehydration experiments were conducted under the protocol described by Churchill and Storey ('94). Individual frogs were weighed and tagged for identification. Frogs were then placed in large desiccators jars (eight to ten frogs per jar). These contained silica gel desiccant on the bottom that was separated from the frogs by a 1-cm thickness of sponge. The jars were held at 5°C and at intervals the frogs were quickly removed and weighed. For *R. sylvatica*, the % H_2O is 80.8 ± 1.2 % (Churchill and Storey, '94). The mean rate of body water loss under these experimental conditions was ~0.5% total body water per hour. Experimental dehydration was continued until the animals reached 40% of total body water lost and then frogs were sampled.

All frogs were euthanized by pithing; tissue samples were rapidly dissected out, immediately frozen in liquid nitrogen, and then stored at −80°C. Protocols for the care, experimentation, and euthanasia of the animals were approved by the Carleton University Animal Care Committee in accordance with the guidelines established by the Canadian Council on Animal Care.

Preparation of Crude Tissue Extracts

Samples of frozen tissue (~500 mg) were placed in 1 mL ice-cold homogenization buffer (20 mM Tris-base, 150 mM NaCl, 1 mM EDTA, 1 mM EGTA, 1 mM NaF, 10 mM ß-glycerophosphate, 1% v:v Triton X-100, and 1 mM phenylmethylsulfonyl fluoride) and immediately homogenized using a Polytron PT-10. Samples were centrifuged for 15 min at 10,000 × *g* at 4°C and supernatants were transferred to clean tubes on ice. Soluble protein concentration was measured using the Coomassie blue dye-binding method with the BioRad prepared reagent (BioRad, Hercules, CA). Following this, the total protein concentration in each sample was normalized to 10 µg/mL by dilution with homogenization buffer. Normalized samples were then mixed 1:1 v:v with SDS-PAGE loading buffer (100 mM Tris–HCl, pH 6.8, 4% w:v SDS, 20% v:v glycerol, 0.2 w:v bromophenol blue, 10% v:v 2-mercaptoethanol) to a final concentration of 5 µg/mL followed by boiling for 5 min. Samples were then stored at −80°C until use.

Immunoblotting

Aliquots containing equal amounts of protein (20 µg) were loaded into wells of 8% SDS-polyacrylamide gels. Electrophoresis was carried out on a Bio-Rad mini-gel apparatus using running buffer (25 mM Tris base, 192 mM glycine, 0.1% w:v SDS, pH 8.3). After electrophoresis, proteins were electroblotted onto polyvinylidene difluoride (PVDF) membrane (Millipore Corporation, Billerica, MA) by wet transfer with prechilled transfer solution (25 mM Tris base pH 8.5, 192 mM glycine, 20% v:v methanol) at 4°C for 1.5 hr at 160 mA. The blots were washed with TBST (Tris-buffered saline containing 0.1% v:v Tween 20, 20 mM Tris base, 140 mM NaCl) for 5 min and were blocked with 100 µg/mL polyvinyl acetate (30–70 kDa) dissolved in TBST on a rocking platform for 45 sec. Blocking solution was decanted, membranes were washed for 2 × 5 min in TBST, and then incubated overnight at 4°C with primary antibodies diluted to 1:1,000 v:v in TBST. After incubation, membranes were washed for 3 × 5 min with TBST and incubated with HRP linked anti-rabbit secondary (1:4,000 v:v dilution in TBST) for 2 hr.

Immunoreactive bands were visualized by enhanced chemiluminescence (Fig. 2) (Millipore Corporation). To confirm equal loading of the lanes, PVDF membranes were stained for 20 min with Coomassie blue protein stain (0.25% w:v Coomassie Brilliant Blue R, 50% v:v methanol, 7.5% v:v acetic acid) and destained for 5–7 min with destaining solution (50 mL distilled water, 50 mL acetic acid, and 150 mL methanol). Rabbit anti-cyclin (types A,B,D, and E) (kit-ab6552) and rabbit anti-cdk (types 4 and 6) (kit-ab6553) polyclonal antibodies were purchased from Abcam (Cambridge, MA); rabbit anti-cdk2 (sc-748), rabbit anti-cdk (Thr14/Tyr15) (sc-28435), and rabbit anti-$p16^{INK4a}$ (sc-28260) polyclonal antibodies were purchased from Santa Cruz Biotechnology (Santa Cruz, CA); rabbit anti-cdk1 (A01295), rabbit anti-p27 (A00436), rabbit anti-cdc25a (A00446), and rabbit

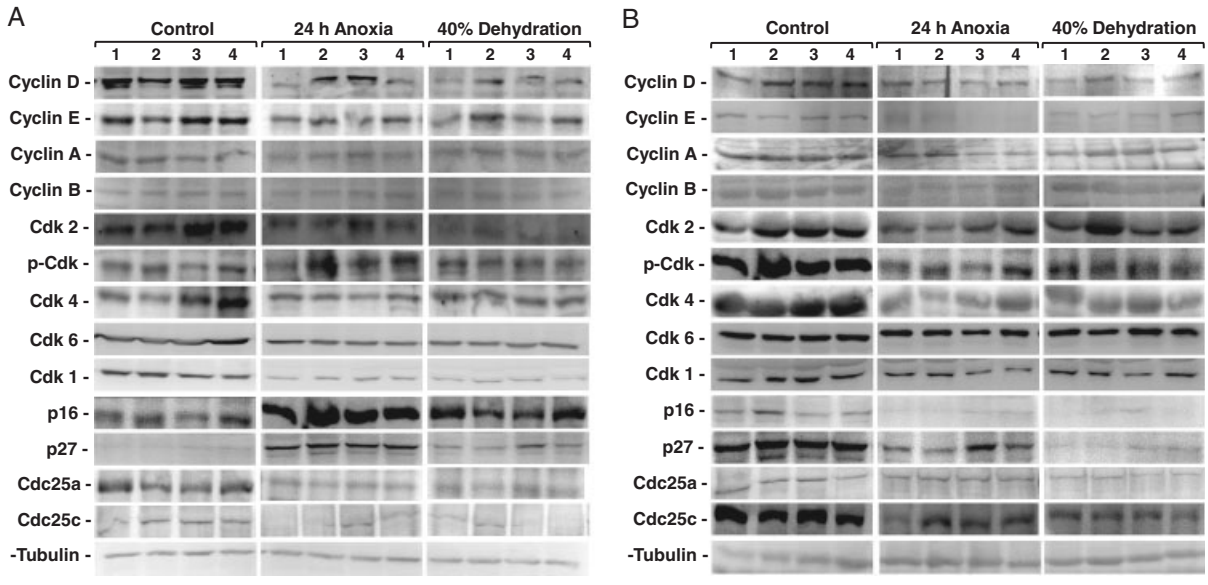

Figure 2. Immunoreactive bands from (A) liver and (B) skeletal muscle tissues in wood frogs. Bands show respective intensity under control conditions, 24 hr anoxia and 40% dehydration stress ($n = 4$ independent trials on tissue from different animals).

anti-cdc25c (A00433) were purchased from GenScript Corporation (Piscataway, NJ). All primary antibodies were raised against mammalian antigens and were diluted in TBST according to the manufacturer's specifications. Mammalian homogenates (*Spermophilus tridecemlineatus*) were used as a positive control for all frog immunoreactive material.

Immunoblotting with α-tubulin-specific antibodies showed constant α-tubulin expression in all experimental conditions (both liver and muscle tissues) and when compared with the combined density of a group of Coomassie stained protein bands. Immunoblots of the proteins of interest were individually adjusted for loading irregularities by normalizing the band intensity of immune-reactive material in each lane against the combined density of a group of Coomassie-stained protein bands in its respective sample lane. These Coomassie-stained proteins showed similar expression pattern to α-tubulin and the same stained bands were used for each such comparison.

Normalization and Statistics

Both immunoblot and Coomassie-stained bands were visualized using a ChemiGenius Bio-Imaging System and densitometric analysis was performed with the associated GeneTools software (Syngene, Frederick, MD). The qualitative comparison of soluble protein, as measured by immunoblotting, is reported as normalized band densities ± SEM for $n = 4$ independent biological samples from different animals for each condition. Statistical testing used the Student's *t*-test.

RESULTS

Cyclin Responses to Anoxia and Dehydration Stresses

Expression levels of cyclin proteins revealed similar regulation in liver (Fig. 3A) and skeletal muscle (Fig. 3B) from frogs in response to 24-hr anoxia exposure. Cyclin D (immoreactive band of 38 kDa) and E (48 kDa) protein decreased significantly under anoxia by 39 and 26% in liver ($P<0.05$) and by 59 and 72% in muscle ($P<0.05$) as compared with corresponding control values. Cyclin A (41 kDa) protein levels were significantly reduced by 34% ($P<0.05$) in liver and 51% ($P<0.05$) in skeletal muscle. Similarly, expression levels of cyclin B (40 kDa) protein also decreased significantly by 54% ($P<0.05$) in liver and 56% ($P<0.05$) in skeletal muscle during anoxia.

Similar to the effect of anoxia stress, the levels of most cyclins also decreased significantly in response to whole body dehydration to 40% of total body water lost. Data for liver are shown in Figure 3A and skeletal muscle in Figure 3B. Levels of cyclin D protein were reduced by 38% ($P<0.05$) in liver and by 63% ($P<0.05$) in skeletal muscle from dehydrated frogs, compared with controls, whereas corresponding reductions in cyclin E levels were 40% ($P<0.05$) and 38% ($P<0.05$), as compared with control values. Cyclin A levels were significantly reduced by 48% in liver ($P<0.05$) and by 33% in skeletal muscle. Cyclin B protein

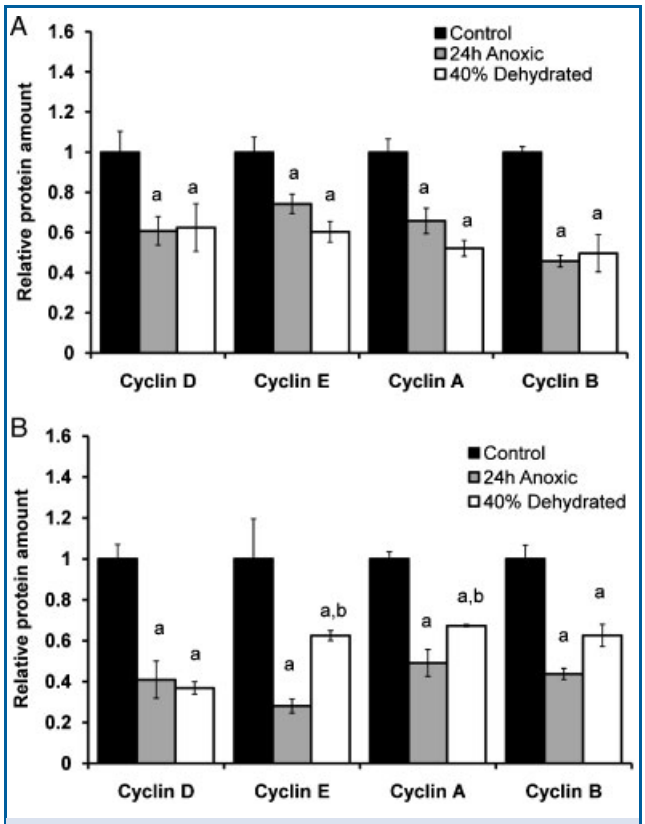

Figure 3. Relative protein expression of cyclin proteins in (**A**) liver and (**B**) skeletal muscle in wood frogs under control conditions, 24 hr anoxia and 40% dehydration stress. Histogram shows normalized protein expression levels for control versus stress conditions; data are means ± SEM ($n = 4$ independent trials on tissue from different animals). Symbols "a and b" indicate significant differences from the control and 24 hr anoxic conditions respectively ($P<0.05$).

content also decreased significantly during dehydration, by 50 and 37% in liver and skeletal muscle, respectively ($P<0.05$).

Cdk Responses to Anoxia Dehydration

Protein levels of most Cdks decreased significantly in response to 24 hr of anoxia exposure in both liver (Fig. 4A) and skeletal muscle (Fig. 4B). Levels of Cdk 2 (32 kDa) decreased significantly by 38% ($P<0.05$) in liver and by 54% ($P<0.05$) in skeletal muscle after 24-hr exposure to anoxia, as compared with control values. Protein levels of both Cdk 4 (36 kDa) and Cdk 6 (40 kDa) also decreased significantly ($P<0.05$) under anoxia by 35 and 53% in the liver and by 38 and 35% in skeletal muscle, respectively. Levels of Cdk 1 (32 kDa) decreased significantly by 49% ($P<0.05$) in liver exposed to 24 hr of anoxia stress, but no significant change was observed in skeletal muscle. To measure the relative amount of inactive Cdk protein, an antibody that

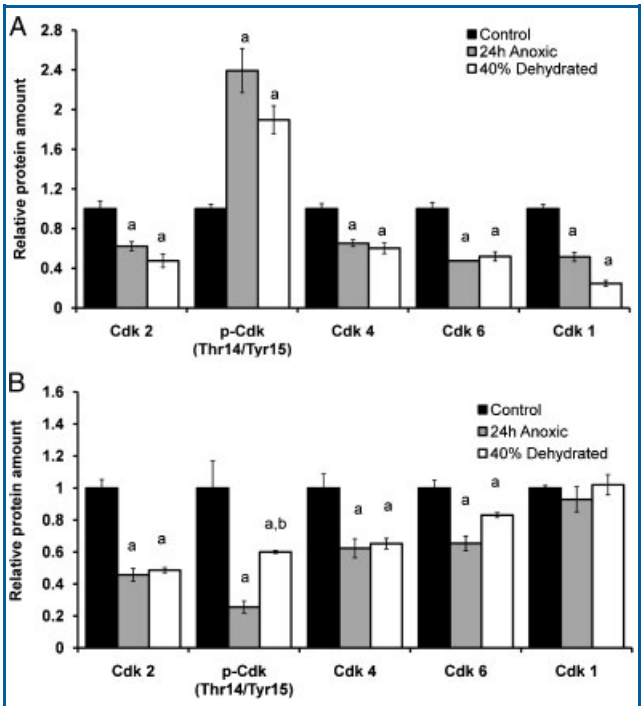

Figure 4. Relative protein expression of Cdk proteins in (A) liver and (B) skeletal muscle in wood frogs under control conditions, 24 hr anoxia and 40% dehydration stress. Histogram shows normalized protein expression levels for control versus stress conditions; data are means ± SEM ($n = 4$ independent trials on tissue from different animals). Symbols "a and b" indicate significant differences from the control and 24 hr anoxic conditions respectively ($P < 0.05$).

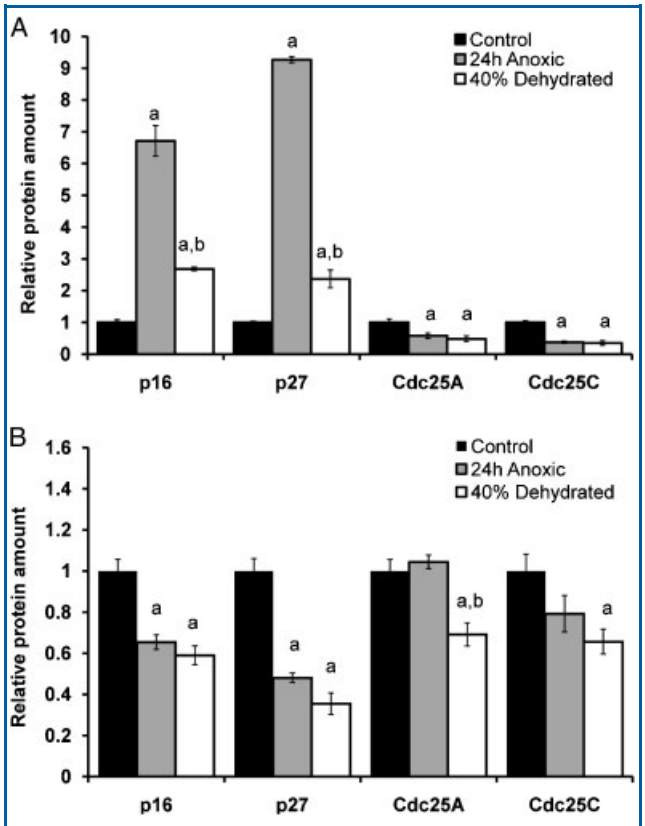

Figure 5. Relative protein expression of Cdk regulator proteins in (A) liver and (B) skeletal muscle in wood frogs under control conditions, 24 hr anoxia and 40% dehydration stress. Histogram shows normalized protein expression levels for control versus stress conditions; data are means ± SEM ($n = 4$ independent trials on tissue from different animals). Symbols "a and b" indicate significant differences from the control and 24 hr anoxic conditions respectively ($P < 0.05$).

recognizes phosphorylated Thr14 and Tyr15, common inhibitory phosphorylation residue on Cdks (type 1 and 2), was used. The relative amount of p-Cdk (Thr14/Tyr15) increased significantly by 2.4-fold ($P < 0.05$) in liver under anoxia, whereas skeletal muscle showed a significant 74% ($P < 0.05$) decrease in p-Cdk content as compared with aerobic control values.

Similar to the response to anoxia, frogs under dehydration stress generally showed reduced Cdk protein levels in both liver (Fig. 4A) and skeletal muscle (Fig. 4B). Protein levels of Cdk 2 decreased significantly by 53% ($P < 0.05$) in liver and by 51% ($P < 0.05$) in skeletal muscle as compared with controls. Both Cdk 4 and Cdk 6 also decreased significantly under dehydration stress by 40 and 48% in liver and by 35 and 17% ($P < 0.05$) in skeletal muscle, respectively. Levels of Cdk 1 also decreased significantly by 75% ($P < 0.05$) in liver from dehydrated but no significant change occurred in skeletal muscle. The relative amount of inactive p-Cdk (Thr14/Tyr15) showed a significant 1.9-fold increase ($P < 0.05$) in liver of dehydrated frogs, whereas in skeletal muscle p-Cdk content decrease significantly by 40% ($P < 0.05$).

Responses of Cdk Regulators to Anoxia and Dehydration Stresses

Positive regulators of Cdk activity, the phosphatases Cdc25A and Cdc25C, showed stress- and tissue-specific regulation between liver (Fig. 5A) and skeletal muscle (Fig. 5B). Anoxia exposure significantly decreased Cdc25A (63 kDa) levels in liver by 42% ($P < 0.05$) from control values, whereas no change occurred in skeletal muscle. Protein levels of Cdc25C (55 kDa) were also reduced in liver by 63% ($P < 0.05$) under anoxia, again with no significant change in skeletal muscle. Similar results were seen for the response of both Cdc25A and Cdc25C to 40% dehydration in liver, with protein content decreasing by 52 and 65% as compared with controls ($P < 0.05$). However, unlike anoxia, dehydration stress significantly decreased Cdc25A levels by 31% ($P < 0.05$) and Cdc25C levels by 36% ($P < 0.05$) in muscle tissue.

Negative regulators of Cdk activity, $p16^{INK4a}$ and $p27^{KIP1}$, also showed specific regulation under both anoxic and dehydration

stresses in both liver (Fig. 5A) and skeletal muscle (Fig. 5B) tissues. Exposure to 24 hr anoxia significantly increased $p16^{INK4a}$ (16 kDa) levels in liver by 6.7-fold ($P<0.05$) as compared with control values, whereas a significant decrease of 35% ($P<0.05$) occurred in skeletal muscle. Similarly, $p27^{KIP1}$ (29 kDa) protein levels in liver increased by 9.3-fold ($P<0.05$) under anoxia but decreased significantly by 52% ($P<0.05$) in skeletal muscle. The response to dehydration stress was similar with $p16^{INK4a}$ and $p27^{KIP1}$ levels in liver increasing by 2.7- and 2.4-fold compared with controls ($P<0.05$). Oppositely, dehydration stress significantly decreased both $p16^{INK4a}$ and $p27^{KIP1}$ in skeletal muscle by 41 and 65% ($P<0.05$), respectively.

DISCUSSION

Cell Cycle Response to Dehydration and Anoxic Stress

The responses of cyclins and Cdks in *R. sylvatica* tissues were similar under both anoxia and dehydration stresses. Under both of these conditions, protein levels of all cyclins, Cdks, and Cdk phosphatases decreased significantly in the liver when compared with control conditions. Similar reductions in the levels of most proteins were seen in skeletal muscle, with the exception of Cdk 1, which displayed no significant changes. Stress-specific responses were only seen with proteins involved in the G_0/G_1-phase of the cell cycle arrest mechanism. This study suggests that anoxia exposure triggers G_0/G_1-phase cell cycle arrest response, likely involving $p16^{INK4a}$, $p27^{KIP1}$, and p-Cdk (Thr14/Tyr15) and the data indicate that this arrest response is more pronounced than the comparable response to dehydration. This result seems plausible given that reversible cell cycle arrest mechanisms have been proposed for many hypoxia-tolerant organisms, including *Caenorhabditis elegans*, *Drosophila melanogaster*, and *Danio rerio* and in these organisms, arrest is thought to occur primarily through entry/exit from the G_0 (Quiescence) phase of the cell cycle (Padilla and Roth, 2001; Padilla et al., 2002; Douglas and Haddad, 2003). Indeed, this mode of cell cycle arrest has also been proposed as a response to anoxia by anoxia-tolerant turtles (*Trachemys scripta elegans*), suggesting that strong suppression of the ATP-expensive cell cycle is a common component of anoxia-induced metabolic rate depression across the animal kingdom (Biggar and Storey, 2009). If these proposals hold true, proteins such as $p16^{INK4a}$ and $p27^{KIP1}$, whose effects are predominately in the G_0/G_1 transition, may play critical roles in coordinating cell cycle arrest mechanisms during hypometabolism.

Indeed, cell cycle arrest responses involving p-Cdk (Thr14/Tyr15), $p16^{INK4a}$, and $p27^{KIP1}$ were activated in response to both anoxia and dehydration stresses in wood frog liver. Levels of Cdk inhibitor proteins, $p16^{INK4a}$ and $p27^{KIP1}$, were strongly elevated in liver under both stresses and the relative amount of phosphorylated inactive Cdks doubled. Another approach has also produced evidence of reversible cell cycle arrest in wood frog liver under stress conditions; this is the differential expression of microRNA species. Levels of one microRNA known to play a critical role in cell cycle arrest, miR-16, increased significantly in liver when wood frogs were frozen (although no changes were seen in skeletal muscle) (Biggar et al., 2009). Similarly, studies examining the involvement of microRNAs in cell cycle regulation in HeLa cells have shown that the overexpression of miR-16 alone was sufficient to induce cell cycle arrest, acting to repress the translation of both cyclin D and Cdk 6 mRNA (Linsley et al., 2007). In the wood frog, changes in the expression of cell cycle components during periods of environmental stress may similarly be linked with the overexpression of miR-16 and may be particularly important in tissues with proliferative potential, such as liver.

Alternate Roles of Cell Cycle Components in Liver and Muscle Tissues

Similar to both liver and muscle tissues, reductions of both cdc25a and cdc25c phosphatases may be a result of decrease in response to an oxidative stress or hypoxia-induced activation of DNA-damage response pathways; ataxia telangiectasia mutated (ATM) and ataxia telangiectasia and Rad3-related protein (ATR). DNA-damage checkpoints ensure the maintenance of genomic integrity during periods of stress and are commonly activated upon cellular exposure to oxidative stress and UV irradiation (Hammond and Giaccia, 2004; Stokes et al., 2007). Such checkpoints comprised apical signal transducing kinases such as phosphatidylinositol 3-kinase (PI3K)-like family members, ATR, and ATM kinases (Falck et al., 2001; Choudhury et al., 2006). These kinases regulate the distal serine/threonine signal transducing kinases, Checkpoints 1 and 2 (Chk1 and Chk2). Interestingly, although hypoxia does not itself induce DNA damage, several studies have indicated the activation of Chk1 and Chk2 in an ATM/ATR-dependant manner in response to both oxidative stress and hypoxia (Hammond et al., 2003; Hammond and Giaccia, 2004; Bencokova et al., 2009). In addition, the activation of ATM/ATR induces the stabilization of p53- and ubiquitination-dependent degradation of both cdc25a and cdc25c. In wood frogs, reperfusion of oxygen after anoxia or dehydration introduces the potential for oxidative damage, similar to the consequence of ischemia-reperfusion injuries seen after a heart attack or stroke in mammals. The state of oxidative stress in wood frogs has been explored by Joanisse and Storey ('96), and examined the effects of freezing exposure (24 hr) on the antioxidant systems of several wood frog. Of particular interest was the increase of ~25 and ~50% in selenium-dependent and selenium-independent glutathione peroxidase (GPX) activity after exposure to 24 hr of freezing in liver and skeletal muscle tissues, respectively (Joanisse and Storey, '96). Interestingly, this study identified that anticipatory increases seen in GPX activity during freezing, may act as a protection mechanism to enhance antioxidant defenses before oxygen reperfusion. Similarly, potential activation of DNA-damage pathways could be a

hypoxia-dependant or perhaps act as an enhanced protection mechanism against oxygen reperfusion. Future studies may identify whether the activation of ATM/ATR is a key mechanism in maintaining genomic integrity during periods of environmental stress in the wood frog.

Apart from the maintenance of genome integrity are the auxiliary roles of both $p16^{INK4a}$ and $p27^{KIP1}$ proteins in the stress response as seen in liver and skeletal muscle tissues. As previously mentioned, typical cell cycle arrest mechanisms, including inhibitory phosphorylation of Cdks, and elevated $p16^{INK4a}$ and $p27^{KIP1}$ proteins, are involved with the establishment of stress tolerance in liver. However, differences between liver and skeletal muscle responses were identified in wood frogs and may be explained by the low proliferative nature of skeletal myocytes. In order to achieve terminal differentiation, skeletal myocytes establish irreversible cell cycle arrest mechanisms making the implementation of a reversible arrest mechanism redundant (Guo et al., '95). However, the ectopic expression of cyclins and associated Cdks under control conditions may act to continuously inhibit myocyte differentiation by repressing gene activation of muscle-specific transcription factors, myogenic differentiation protein (MyoD) and myogenin. This repression is established by a mechanism independent of the cell cycle and is thought to involve inhibitory phosphorylation of both MyoD and myogenin by cyclin:Cdk complexes (Skapek et al., '96). Reduced levels of cyclin and Cdk proteins in muscle under anoxia or dehydration stresses may indicate a relief of this repression, allowing for the increased expression of MyoD and myogenin downstream targets. One pertinent target regulated by MyoD is creatine kinase, an enzyme known to be regulated post-translationally in the wood frog during freezing and which is a key contributor to maintaining energy homeostasis by buffering the intracellular ATP/ADP ratio (Dieni and Storey, 2009). Another target of MyoD is the myocyte enhancer factor-2, a major regulatory protein that contributes to muscle remodeling and the establishment of antiapoptotic processes (Black and Olson, '98; Potthoff and Olson, 2007). Enhancement of antiapoptotic processes may be particularly important for animals in hypometabolic states; ATP-expensive processes including transcription, translation, and protein degradation are strongly suppressed during torpor and therefore cytoprotective mechanisms come to the forefront to extend the lifespan of cells and their macromolecules. The suppression of selected cell cycle proteins under stress conditions may, therefore, have the consequence of enhancing antiapoptotic mechanisms and thereby contribute to myocyte survival during prolonged periods of hypometabolism.

In summary, this study provides the first demonstration of cell cycle regulation in an anoxia- and dehydration-tolerant vertebrate animal. *R. sylvatica* provides an excellent model system for studying the responses of cell cycle processes to both anoxic and dehydration stress. Regulation of this pathway may have profound implications for energy homeostasis in the hypometabolic state by helping to inhibit ATP usage by nonessential energy-expensive cell functions including cell growth, division and replacement, as well as apoptosis. Although the full mechanism of cell cycle maintenance in stress-induced hypometabolic states remains to be elucidated, this study suggests that the cell cycle inhibitors, $p16^{INK4a}$ and $p27^{KIP1}$, have major roles to play in the regulation of organ-specific responses to both anoxic and dehydration stresses. The current research also provides many new and exciting questions regarding both generalized processes and mechanisms of arrest contributing toward an overall suppression of metabolic rate in vertebrate organisms. Continuing research on the wood frog will most certainly demonstrate the molecular mechanisms underlying the survival response to both anoxia and dehydration.

ACKNOWLEDGMENTS

Thanks to J.M. Storey for editorial review of the manuscript. Supported by a discovery grant from the Natural Sciences and Engineering Research Council (NSERC) of Canada (6793). K.B.S. holds the Canada Research Chair in Molecular Physiology; K.K.B. held a NSERC postgraduate fellowship.

LITERATURE CITED

Bencokova Z, Kaufmann M, Pires I, Lecane P, Giaccia A, Hammond EM. 2009. ATM activation and signaling under hypoxia conditions. Mol Cell Biol 29:526–537.

Biggar KK, Storey KB. 2009. Perspectives in cell cycle regulation: lessons from an anoxic vertebrate. Curr Genomics 10:573–584.

Biggar KK, Dubuc A, Storey KB. 2009. MicroRNA regulation below zero: differential expression of miRNA-21and miRNA-16 during freezing in wood frogs. Cryobiology 59:317–321.

Black B, Olson EN. 1998. Transcriptional control of muscle development by myocyte enhancer factor-2 (MEF2) proteins. Annu Rev Cell Dev Biol 14:167–196.

Choudhury A, Cuddihy A, Bristow R. 2006. Radiation and new molecular agents Part I: target ATM-ATR checkpoints, DNA repair, and the proteasome. Semin Radiat Oncol 16:51–58.

Churchill TA, Storey KB. 1994. Metabolic responses to dehydration by liver of the wood frog, *Rana sylvatica*. Can J Zool 72:1420–1425.

Dalal S, Bruera E. 2004. Dehydration in cancer patients: to treat of not to treat. J Support Oncol 2:467–487.

Dieni CA, Storey KB. 2009. Creatine kinase regulation by reversible phosphorylation in frog muscle. J Comp Physiol [B] 152:405–412.

Douglas R, Haddad G. 2003. Effect of oxygen deprivation on cell cycle activity: a profile of delay and arrest. J Appl Physiol 94:2068–2083.

Falck J, Mailand N, Syljuasen RG, Bartek J, Lukas J. 2001. The ATM-Chk2-Cdc25a checkpoint pathway guards against radioresistant DNA synthesis. Nature 410:842–847.

Guo K, Wang J, Andres V, Smith RC, Walsh K. 1995. MyoD-induced expression of p21 inhibits cyclin-dependent kinase activity upon myocyte terminal differentiation. Mol Cell Biol 15:3823–3829.

Guardavaccaro D, Pagano M. 2006. Stabilizers and destabilizers controlling cell cycle oscillators. Mol Cell 22:1–4.

Hammond EM, Giaccia AJ. 2004. The role of ATM and ATR in the cellular response to hypoxia and re-oxygenation. DNA Repair 3: 1117–1122.

Hammond EM, Dorie MJ, Giaccia AJ. 2003. ATR/ATM targets are phosphorylated by ATR in response to hypoxia and ATM in response to reoxygenation. J Biol Chem 278:12207–12213.

Harrisingh MC, Perez-Nadales E, Parkinson DB, Malcolm DS, Mudge AW, Lloyd AC. 2004. The Ras/Raf/ERK signalling pathway drives Schwann cell differentiation. EMBO J 23:3061–3071.

Hillman SS, Withers PC, Drewes RC, Hillyard SD. 2009. Ecological and environmental physiology of amphibians. Oxford: Oxford University Press.

Holden CP, Storey KB. 1997. Second messenger and cAMP-dependent protein kinase responses to dehydration and anoxia stresses in frogs. J Comp Physiol [B] 167:305–312.

Joanisse DR, Storey KB. 1996. Oxidative damage and antioxidants in *Rana sylvatica,* the freeze tolerant wood frog. Am J Physiol 271: R545–R553.

Linsley P, Schelter J, Burchard J, Kibukawa M, Martin M, Bartz S, Johnson J, Cummins J, Raymond C, Dai H, Chau N, Cleary N, Jackson A, Carleton M, Lim L. 2007. Transcripts targeted by the microRNA-16 family cooperatively regulate cell cycle progression. Mol Cell Biol 27:2240–2252.

Mazia D. 1962. Biochemistry of the dividing cell. Annu Rev Biochem 30:669–688.

Obaya A, Sedivy J. 2002. Regulation of cyclin-cdk activity in mammalian cells. Cell Mol Life Sci 59:126–142.

Padilla PA, Roth MB. 2001. Oxygen deprivation causes suspended animation in the zebrafish embryo. Proc Natl Acad Sci USA 98: 7331–7335.

Padilla PA, Nystul TG, Zager RA, Johnson AC, Roth MB. 2002. Dephosphorylation of cell cycle-reulated proteins correlates with anoxia-induced suspended animation in *Caenorhabditis elegans*. Mol Biol Cell 13:1473–1483.

Pavletich N. 1999. Mechanisms of cyclin-dependent kinase regulation: structures of Cdks, their cyclin activators, and Cip and INK4 inhibitors. J Mol Biol 287:821–828.

Potthoff MJ, Olson EN. 2007. MEF2: a central regulator of diverse developmental programs. Development 134:4131–4140.

Semenza GL. 2007. Hypoxia and cancer. Cancer Metastasis Rev 26: 223–224.

Skapek SX, Rhee J, Kim PS, Novitch BG, Lassar AB. 1996. Cyclin-mediated inhibition of muscle gene expression via a mechanism that is independent of pRB hyperphosphorylation. Mol Cell Biol 16: 7043–7053.

Stokes MP, Rush J, Macneill J, Ren JM, Sprott K, Nardone J, Yang V, Beausoleil SA, Gygi SP, Livingstone M, Zhang H, Polakiewicz RD, Comb MJ. 2007. Profiling of UV-induced ATM/ATR signaling pathways. Proc Natl Acad Sci USA 104:19855–19860.

Storey KB, Storey JM. 2004a. Physiology, biochemistry and molecular biology of vertebrate freeze tolerance: the wood frog. In: Benson E, Fuller B, Lane N, editors. Life in the frozen state. Boca Raton: CRC Press. p 243–274.

Storey KB, Storey JM. 2004b. Metabolic rate depression in animals: transcriptional and translational controls. Biol Rev Camb Philos Soc 79:207–233.

Storey KB, Storey JM. 2007. Putting life on ''pause''—molecular regulation of hypometabolism. J Exp Biol 210:1700–1714.

Welburn J, Tucker J, Johnson T, Lindert L, Morgan M, Willis W, Noble E, Endicott AJ. 2007. How tyrosine 15 phosphorylation inhibits the activity of cyclin-dependent kinase 2-cyclin A. J Biol Chem 282: 3173–3181.